

Vortex Activation Energy and Normalized Magnetization Relaxation Rate in the $\text{YBa}_2\text{Cu}_3\text{O}_{7-\delta}/\text{YSZ}$ Quasi-multilayer

L. Peng · Y. Liu · T. Gao · C. Cai · J. Zhang

Received: 4 November 2010 / Accepted: 29 November 2010 / Published online: 22 December 2010
© Springer Science+Business Media, LLC 2010

Abstract The quasi-multilayer films of $\text{YBa}_2\text{Cu}_3\text{O}_{7-\delta}/\text{YSZ}$ are prepared by means of pulsed laser deposition (PLD) and a systematic study of I – V characteristic curves for the YBCO/YSZ quasi-multilayer film are presented, with magnetic fields up to 7 T and $15 \text{ K} < T < 80 \text{ K}$. The activation energy $E(H, T)$ for flux line depinning is determined by fitting the nonlinear of the curves up to the flux flow region. And magnetization relaxation rate $S(T)$ is also approximately obtained by a convenient way. The results show the $S(T)$ plateau-like domain for the $\text{YBa}_2\text{Cu}_3\text{O}_{7-\delta}/\text{YSZ}$ quasi-multilayer film develops at high H ($\sim 7 \text{ T}$) at intermediate temperatures $25 \text{ K} < T < 55 \text{ K}$, while the $S(T)$ plateau-like domain for the optimally doped $\text{YBa}_2\text{Cu}_3\text{O}_{7-\delta}$ films disappears at $H = 2 \text{ T}$, which implies the defects introduced in the quasi-multilayer serve as strong pinning centers and influence the thermal activated state of the system at low bias current values.

Keywords I – V characteristic · Activation energy · Magnetization relaxation rate

1 Introduction

The epitaxial thin-film structure of the high- T_c superconductor $\text{REBa}_2\text{Cu}_3\text{O}_{7-\delta}$ (REBCO, RE = Y, Nd, Sm, etc. rare earths) allows generation of the high critical current

densities, although the vortex-pinning mechanism remains controversial. These current densities indicate that a large amount of correlated defects is present in thin films, providing for strong vortex pinning [1–4]. A few groups have made great efforts to improve the flux pinning properties in REBCO thin films. Columnar defects produced by irradiation or extended linear defects incited by miscut substrates can act as the strongest artificial pinning centers [5–7]. Recently, a few other artificial routes, such as rare-earth mixing [8–12], substrate decoration [13, 14], and quasi-multilayer structure [15–19], are also developed to increase flux pinning behaviors for REBCO films. All these defects produced introduced by the methods above act as vortex pinning centers in REBCO films, even though they have different strengths and relevance, and influence the static and dynamic magnetic properties.

For the investigation of vortex dynamics of high-temperature superconductors (HTSs), however, the relaxation of the irreversible magnetization is an essential tool. The understanding of magnetic relaxation in HTSs can contribute to the broader understanding of the pinning mechanisms and to an improved determination of the thermodynamic properties of high-temperature superconductors [20, 21]. For disordered HTSs, the magnetization relaxation rate $S(T)$ exhibits a plateau-like effect which is associated with the existence of an elastic vortex glass, and disappears at high H [20–24]. In this work, we discuss the vortex dynamics of a superconducting quasi-multilayer film through a detailed analysis of magnetization relaxation. The quasi-multilayer structure investigated is built up by using pulsed laser deposition (PLD), which consists of $\text{YBa}_2\text{Cu}_3\text{O}_{7-\delta}$ (YBCO) and Ytria Stabilized Zirconia (YSZ), where the doping phase, YSZ is a widely used substrate or buffer layer material for YBCO film, having a matchable lattice constant with YBCO. During the laser deposition, several pulses on the YSZ target

L. Peng (✉) · Y. Liu · T. Gao
Department of Mathematics and Physics,
Shanghai University of Electric Power, Shanghai, 200090, China
e-mail: plpeng@shu.edu.cn

C. Cai · J. Zhang
Department of Physics, Shanghai University, Shanghai, 200444,
China

give no rise to a complete layer of heterogeneous phases. This results in a so-called “YBCO/YSZ quasi-multilayer”, consisting of YBCO film matrix and the island-like nanoparticles. The results show the appearance of the plateau in $S(T)$ at high H , which is directly related to a crossover in the vortex-creep process generated by the thermal fluctuation and the macroscopic currents induced in the system.

2 Experimental Details

A series of quasi-multilayer films of $p \times (m \text{ YBCO}/n \text{ YSZ})$ were prepared by means of on-axis pulsed-laser deposition using a commercial stoichiometric YBCO target and a YSZ target onto (100) SrTiO₃ single-crystal substrates, where m, n denoted the number of laser pulses on YBCO and YSZ, respectively, and p was the periodic number. A Lambda Physik KrF excimer laser ($\lambda = 248 \text{ nm}$) run at a repetition rate of 5 Hz with an energy density of 2.4–3.0 J/cm² on the target. It was observed that the T_c decreased and the transition width broadened with increasing YSZ doping content. So we focused on the quasi-multilayer film with relatively lower doping contents such as $m = 40, n = 2$, and $p = 70$. Further details about growth and structure could be found elsewhere [18, 19].

Crystallinity and texture were characterized by x-ray diffraction (XRD) with the aid of JADE 6.0 software. The typical $\theta-2\theta$ XRD pattern (Cu $K\alpha_1$, $\lambda = 1.5406 \text{ \AA}$) of a YBCO/YSZ quasi-multilayer revealed that the epitaxial c -axis orientation perpendicular to the plane of the substrate was achieved. In the YBCO/YSZ quasi-multilayer, a chemical reaction takes place, leading to a heterogeneous perovskite phase of BaZrO₃. It was also observed that large particles with a size of more than 50 nm were scattered in the quasi-multilayer by Atomic Force Microscopy (AFM). Transmission Electron Microscopy (TEM) showed the more detailed microstructures such as the planar defects or the nanometer-sized precipitates (correlative defects). The experimental details about these situations above can be found in our previous work [18, 19].

$I-V$ characteristics were measured in various magnetic fields (Quantum Design PPMS) by the standard four-probe method on a bridge of 0.8 mm length and 50 μm width, patterned by photolithography. Magnetic field dependence of $I-V$ curves was measured in the magnetic fields of 0–9 T with the direction parallel to the c -axis and normal to the current flowing direction.

3 Results and Discussion

The $I-V$ characteristics of the YBa₂Cu₃O_{7- δ} /YSZ ($T_c = 87.5 \text{ K}$) quasi-multilayer has been measured by a four-contact method on patterned lines at various magnetic fields

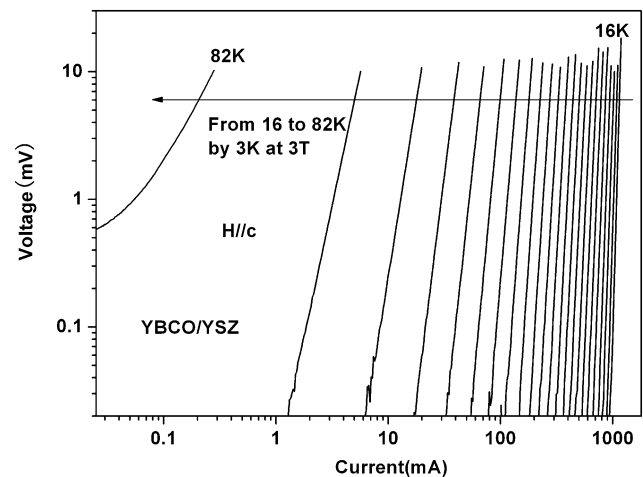


Fig. 1 Magnetotransport measurement for patterned YBCO/YSZ quasi-multilayer films: double logarithmic plots of voltage vs. current at 3 T for various temperatures

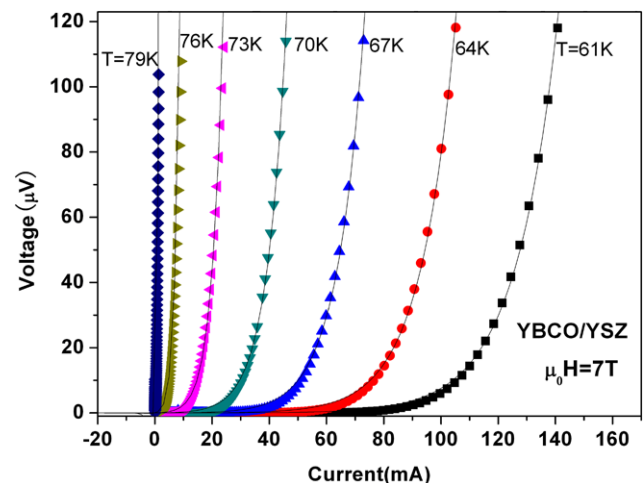


Fig. 2 (Color online) Experimental $I-V$ curves measured for patterned YBCO/YSZ quasi-multilayer films with $H = 7 \text{ T}$ and $61 \text{ K} \leq T \leq 79 \text{ K}$. The temperature step between the selected curves in the graph is 3 K. The continuous lines are fittings according to the vortex activation model

and temperatures. Figure 1 shows a series of isothermal $I-V$ curves. These were measured with temperature variation at a fixed applied field $H = 3 \text{ T}$, which are plotted in double logarithmic scale. The $I-V$ characteristic curves indicate a power-law behavior, representing vortex creep effects at currents very close to or above the critical current. A similar behavior was also observed for other measured magnetic fields.

Figure 2 shows a set of experimental $I-V$ curves measured for $H = 7 \text{ T}$. The continuous lines are fittings described below. The nonlinear region of the experimental $I-V$ curves was fitted from the voltage value correspond-

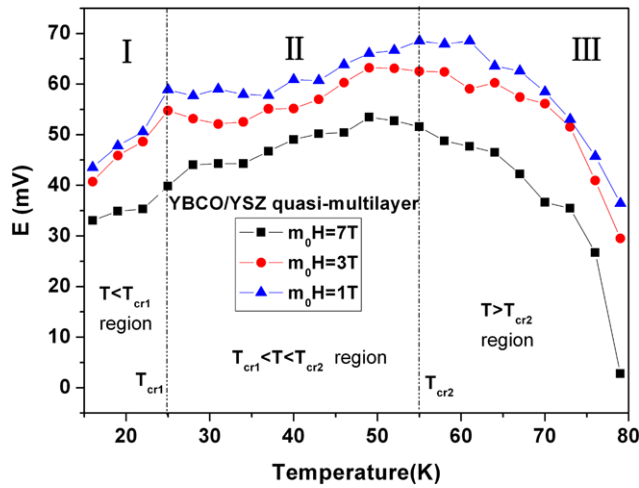


Fig. 3 (Color online) Temperature dependence of the vortex-creep activation energy $E(H, T)$ for different applied fields. $H = 1, 3$ and 7 T. $E(H, T)$ was extracted with the I – V characteristics by fitting the non-linear of the curves up to the vortex flow region, showing a maximum at the crossover temperature T_{cr2}

ing to the J_c criterion up to the linear behavior using the well known expression [21, 25],

$$V(I, H, T) = \alpha I \exp[E(I, H, T)/kT], \tag{1}$$

where I is the applied current, k is the Boltzmann constant, α is a constant, and $E(I, H, T)$ is the current and applied magnetic field dependent activation energy. The parameter (αI) allows a continuous transition to the vortex regime. The activation energy could be assumed to vary linearly with I , and it was written as follows [21]:

$$E(I, H, T) = E(H, T)(1 - I/I_0). \tag{2}$$

An alternative dependence, $E_a \propto \ln(1 - I/I_0)$, leading to unsatisfactory fittings. For a fixed magnetic field, the activation energy $E(H, T)$ is evaluated from the fit parameter I_0 , using the expression above. $E(H, T)$ is sometimes called “the effective pinning energy.” While it cannot actually be identified with the effective pinning barrier, this is very useful for detecting changes in the vortex-creep to vortex-flow crossover process.

For three fixed magnetic fields ($H = 1, 3$ and 7 T), the $E(H, T)$ values for a set of curves are determined and plot as a function of temperature, as shown in Fig. 3. The $E(H, T)$ variation within the range of higher magnetic field (such as 7 T) shows three distinct regions. At the crossover temperature $T_{cr2} \approx 55$ K, $E(H, T)$ exhibits a maximum, which indicates a crossover from vortex-creep to vortex-flow behavior. For $T > T_{cr2}$, $E(H, T)$ shows a sharp decrease, which is mainly caused by the increased thermal fluctuations and the macroscopic current induced in the YBCO/YSZ sample. At the crossover temperature $T_{cr1} \approx 25$ K, $E(H, T)$

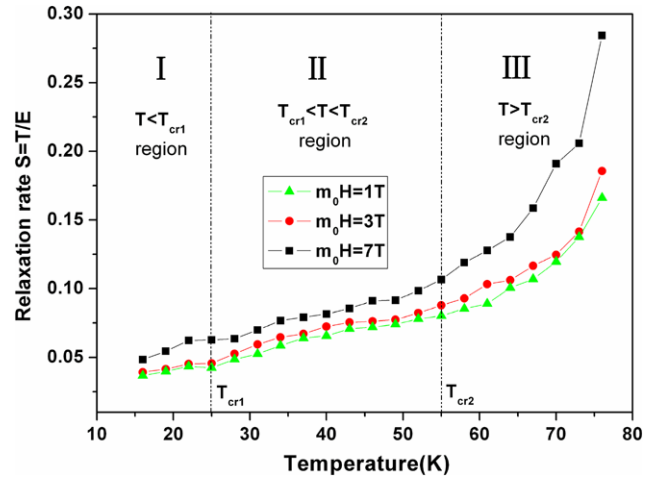


Fig. 4 (Color online) Temperature variation in the normalized magnetization relaxation rate $S(T) = T/E$ for different applied fields. $H = 1, 3$ and 7 T. At high $H = 7$ T the $S(T)$ plateau-like domain was observed, and was located just below the crossover temperature T_{cr2}

shows the vortex change in the quantum creep to vortex creep process. The situation that $T < T_{cr1}$ corresponds to the quantum creep, while the situation that $T_{cr1} < T < T_{cr2}$ corresponds to vortex creep process. For the latter, $E(H, T)$ rises monotonously with the increasing T , and at this case the vortex creep is entirely elastic since some defects may heal and the others will be collectively pinned [21, 24].

For the investigation of vortex dynamics of high-temperature superconductors (HTSs), however, one tends to use the normalized magnetization relaxation rate to describe the vortex-creep behavior and usually determines a normalized magnetization relaxation rate averaged over a fixed relaxation-time window,

$$S = -d \ln(|M|)/d \ln(t), \tag{3}$$

where M is the irreversible magnetization and proportional to the current density J of the macroscopic current, and t is the relaxation time. There are, however, a few drawbacks in using this method to determine the relaxation rate in thin films at different temperatures. At low temperatures, the relaxation is expected to be slow and the relaxation measurements probe the initial process. On the other hand, at high temperatures the decay is fast and for the fixed experimental time window only the “tail” of the relaxation process is measured. So, we avoid the experimental measurement and seek tentatively another convenient way to determine S . Following [24], the related normalized vortex-creep activation energy could be written as

$$E = -T d \ln(t)/d \ln(|M|). \tag{4}$$

According to (3) and (4), the relationship between E and S can be obtained, $S = T/E$. If the activation energy E is known, S can be obtained.

In the case of HTSs with relevant random quenched disorder, the $S(T)$ variation at relatively low H exhibits three distinct regions [21–24]. At high T , $S(T)$ increases with increasing T . At intermediate T values a approximate plateau in $S(T)$ develops, whereas at low T a slight decrease in $S(T)$ with decreasing T appears. The apparent $S(T)$ universality in the plateau-like region is considered as the existence of elastic vortex glass [26]. Nevertheless, the $S(T)$ plateau-like domain shrinks with increasing H , and the $S(T)$ plateau-like domain will disappear at high H (such as $H = 2$ T), even in optimally doped YBCO films [24]. The $S(T)$ variation for the YBCO/YSZ quasi-multilayer film at $H = 1, 3$ and 7 T is plotted in Fig. 4. Figure 4 shows broad plateau-like domain effect, even at high applied field $H = 7$ T. At the lower temperatures ($T < 25$ K) $S(T)$ bends down toward $T = 0$ K, which corresponds to a approximate constant relaxation rate $S(T)$ due to quantum creep. At intermediate temperatures ($25 \text{ K} < T < 55 \text{ K}$) $E(H, T)$ rises monotonously and the $S(T)$ plateau-like develops. At higher temperatures, however, the $S(T)$ increases exponentially due to the effect of thermal fluctuations and macroscopic current induced in the YBCO/YSZ quasi-multilayer film, which results in a sharp decrease of $E(H, T)$. Compared with optimally doped YBCO films (see [24]), the $S(T)$ plateau-like effect at high H implies the correlative defects introduced in the quasi-multilayer serve as strong pinning centers, promote the localization of the flux lines, and delay the transition from vortex-creep to vortex-flow process. It is demonstrated that our growth control strategy is very effective in preventing the vortex motion at high fields and high temperatures.

4 Conclusion

The quasi-multilayer films of YBCO/YSZ are prepared by means of pulsed laser deposition (PLD) and a detailed investigation of I – V characteristic curves in the YBCO/YSZ quasi-multilayer films are presented. Information on the quasi-multilayer film pinning and vortex-creep process can be extracted, by the analysis of the I – V characteristic at high H . The normalized magnetization relaxation $S(T)$ for the quasi-multilayer films exhibits apparently the plateau-like behavior at the intermediate T range and the high H , associated with the presence of elastic vortex creep. This shows the defects introduced in the quasi-multilayer serve as strong pinning centers, promote the localization of the flux lines, and impede the transition from vortex-creep to vortex-flow process.

Acknowledgements This work is partly sponsored by the National Natural Science Foundation of China (No. 10804072), the Science and Technology Commission of Shanghai Municipality (Nos.

0952nm02700, 08JC1410400, 07QA14026), the Innovation Program of Shanghai Municipal Education Commission (No. 11ZZ168), and one of authors (Lin Peng) acknowledges the project of the young teachers fund of Shanghai University of Electric Power, China.

References

- Joos, C., Warthmann, R., Kronmüller, H.: Phys. Rev. B **61**, 12433 (2000)
- Parans Paranthaman, M., Izumi, T.: Mater. Res. Soc. Bull. **29**, 533 (2004)
- Dam, B., Huijbregtse, J.M., Klaassen, F.C., van der Geest, R.C.F., Doornbos, G., Rector, J.H., Testa, A.M., Freisem, S., Martinez, J.C., Stäuble-Pümpin, B., Griessen, R.: Nature **399**, 439 (1999)
- Gutiérrez, J., Llordés, A., Gazquez, J., Gibert, M., Roma, N., Ricart, S., Pomar, A., Sandiumenge, F., Mestres, N., Puig, T., Obradors, X.: Nat. Mater. **6**, 367 (2007)
- Gerhauser, W., Ries, G., Neumüller, H.W., Schmidt, W., Eibl, O., Ischenko, S., Klaumunzer, S.: Phys. Rev. Lett. **68**, 879 (1992)
- Thompson, J.R., Wheeler, R., Marwick, A.D., Lisowski, P.: Appl. Phys. Lett. **64**, 3331 (1994)
- Lowndes, D.H., Christen, D.K., Klabunde, C.E., Wang, Z.L., Kroeger, D.M.: Phys. Rev. Lett. **74**, 2355 (1995)
- MacManus-Driscoll, J.L., Foltyn, S.R., Jia, Q.X., Wang, H., Serquis, A., Maiorov, B., Civale, L., Lin, Y., Hawley, M.E., Maley, M.P., Peterson, D.E.: Appl. Phys. Lett. **84**, 5329 (2004)
- MacManus-Driscoll, J.L., Foltyn, S.R., Jia, Q.X., Wang, H., Serquis, A., Civale, L., Maiorov, B., Hawley, M.E., Maley, M.P., Peterson, D.E.: Nat. Mater. **3**, 439 (2004)
- Gutiérrez, J., Puig, T., Obradors, X.: Appl. Phys. Lett. **90**, 162514 (2007)
- Gutiérrez, J., Llordés, A., Gázquez, J., Gibert, M., Romá, N., Ricart, S., Pomar, A., Sandiumenge, F., Puig, T., Obradors, X.: Nat. Mater. **6**, 367 (2007)
- Maiorov, B., Baily, S.A., Zhou, H., Ugurlu, O., Kennison, J.A., Dowden, P.C., Holesinger, T.G., Foltyn, S.R., Civale, L.: Nat. Mater. **8**, 367 (2009)
- Matsumoto, K., Horide, T., Osamura, K., Mukaida, M., Yoshida, Y., Ichinose, A., Horii, S.: Physica C **412**, 1267 (2004)
- Matsumoto, K., Horide, T., Ichinose, A., Horii, S., Yoshida, Y., Mukaida, M.: Jpn. J. Appl. Phys. **44**, L246 (2005)
- Cai, C., Holzapfel, B., Hänisch, J., Schultz, L.: Phys. Rev. B **70**, 212501 (2004)
- Cai, C., Holzapfel, B., Hänisch, J., Fernandez, L., Schultz, L.: Appl. Phys. Lett. **84**, 377 (2004)
- Haugan, T., Barnes, P.N., Wheeler, R., Meisenkothen, F., Sumpston, M.: Nature (Lond.) **430**, 867 (2004)
- Peng, L., Cai, C., Chen, C., Liu, Z., Liu, J., Gao, B., Zhang, J.: J. Phys. D, Appl. Phys. **41**, 155403 (2008)
- Peng, L., Cai, C., Chen, C., Liu, Z., Hühne, R., Holzapfel, B.: J. Appl. Phys. **104**, 033920 (2008)
- Klaassen, F.C., Doornbos, G., Huijbregtse, J.M., van der Geest, R.C.F., Dam, B., Griessen, R.: Phys. Rev. B **64**, 184523 (2004)
- Yeshurun, Y., Malozemoff, A.P., Shaulov, A.: Rev. Mod. Phys. **68**, 911 (1996)
- Malozemoff, A.P., Fisher, M.P.A.: Phys. Rev. B **42**, 6784 (1990)
- Campbell, I.A., Fruchter, L., Cabanel, R.: Phys. Rev. Lett. **64**, 1561 (1990)
- Miu, L., Miu, D., Petrisor, T., Tahan, E.A., Jakob, G., Adrian, H.: Phys. Rev. B **78**, 212508 (2008)
- García, S., Ghivelder, L.: Phys. Rev. B **70**, 052503 (2004)
- Fisher, D.S., Fisher, M.P.A., Huse, D.A.: Phys. Rev. B **43**, 130 (1991)